

# Volcanic plume height correlated with magma-pressure change at Grímsvötn Volcano, Iceland

Sigrún Hreinsdóttir<sup>1</sup>\*, Freysteinn Sigmundsson<sup>1</sup>\*, Matthew J. Roberts<sup>2</sup>, Halldór Björnsson<sup>2</sup>, Ronni Grapenthin<sup>3</sup>†, Pórdur Arason<sup>2</sup>, Thóra Árnadóttir<sup>1</sup>, Jósef Hólmjárn<sup>2</sup>, Halldór Geirsson<sup>4</sup>, Richard A. Bennett<sup>5</sup>, Magnús T. Gudmundsson<sup>1</sup>, Björn Oddsson<sup>1</sup>, Benedikt G. Ófeigsson<sup>1,2</sup>, Thierry Villemain<sup>6</sup>, Thorsteinn Jónsson<sup>1</sup>, Erik Sturkell<sup>7</sup>, Árman Höskuldsson<sup>1</sup>, Guðrún Larsen<sup>1</sup>, Thor Thordarson<sup>1</sup> and Bergrún Arna Óladóttir<sup>1</sup>

**Magma flow during volcanic eruptions causes surface deformation that can be used to constrain the location, geometry and internal pressure evolution of the underlying magmatic source<sup>1</sup>. The height of the volcanic plumes during explosive eruptions also varies with magma flow rate, in a nonlinear way<sup>2,3</sup>. In May 2011, an explosive eruption at Grímsvötn Volcano, Iceland, erupted about 0.27 km<sup>3</sup> dense-rock equivalent of basaltic magma in an eruption plume that was about 20 km high. Here we use Global Positioning System (GPS) and tilt data, measured before and during the eruption at Grímsvötn Volcano, to show that the rate of pressure change in an underlying magma chamber correlates with the height of the volcanic plume over the course of the eruption. We interpret ground deformation of the volcano, measured by geodesy, to result from a pressure drop within a magma chamber at about 1.7 km depth. We estimate the rate of magma discharge and the associated evolution of the plume height by differentiating the co-eruptive pressure drop with time. The time from the initiation of the pressure drop to the onset of the eruption was about 60 min, with about 25% of the total pressure change preceding the eruption. Near-real-time geodetic observations can thus be useful for both timely eruption warnings and for constraining the evolution of volcanic plumes.**

Grímsvötn is a subglacial basaltic volcano beneath the Vatnajökull ice cap, Iceland (Fig. 1). It hosts a caldera complex where a geothermal area<sup>4</sup> melts ice and sustains a subglacial caldera lake. The volcano has a low seismic velocity anomaly down to ~3 km depth interpreted as a magma chamber<sup>5</sup>, and a deeper intrusive complex inferred from a gravity high<sup>6</sup>. Grímsvötn is Iceland's most frequently erupting volcano where magma–ice interaction leads to phreatomagmatic activity. The most recent eruptions occurred in 1983, 1998, 2004<sup>7</sup> and 2011. One nunatak, Mount Grímsfjall, protrudes from the ice at the southern rim of the caldera where a seismometer, a GPS station and a tiltmeter are located. GPS measurements have been conducted intermittently since 1992 and continuously since 2004<sup>8,9</sup>. In addition to glacio-isostatic uplift in response to the melting of the Vatnajökull ice cap, the measurements reveal uplift and displacement away from the caldera between eruptions, interrupted by sudden co-eruptive subsidence

and displacement towards the caldera. This inflation/deflation pattern suggests deformation driven by pressure change in an upper crustal magma chamber, similar to other highly active calderas in Iceland such as Askja and Krafla<sup>10</sup>.

The 21–28 May 2011 eruption was Grímsvötn's largest since 1873, with a Volcanic Explosivity Index (VEI) of magnitude 4. Extensive ash fallout occurred in southeast Iceland. The eruption plume caused airspace closures in northern Europe and the cancellation of about 900 passenger flights. The eruption was preceded by inflation of the volcano since the 2004 eruption and a progressive increase in seismicity. On 21 May an earthquake swarm began at about 17:50 utc, followed by a seismic tremor and eruption onset from a short fissure at around 19:00 (Supplementary Fig. 1). The eruption deposited a southward-trending tephra layer, decreasing in thickness from 170 cm at 7 km distance to 10 cm at 35 km distance from the vent. By mapping the tephra layer on land (~75% of total volume) and extrapolating out to sea by assuming an exponential decline in thickness, we estimate a total erupted volume of  $0.27 \pm 0.07$  km<sup>3</sup> dense-rock equivalent (DRE; using tephra and DRE densities of 1,000 and 2,700 kg m<sup>-3</sup> respectively).

Kinematic 1 Hz solutions were derived for the position of the GPS station GFUM on Mount Grímsfjall, located ~6 km from the eruptive vents, in the hours immediately before and during the 2011 Grímsvötn eruption (Fig. 1). Recordings of ground tilt supplement the GPS data. The onset of deformation preceded the eruption by one hour and throughout the eruption GFUM moved consistently in direction  $N38.4 \pm 0.5^\circ$  W (Figs 1 and 2 and Supplementary Information), opposite to the direction of movements during the 2004–2011 inter-eruptive phase<sup>8,9</sup>. The maximum change associated with the eruption was  $u_r = 513 \pm 4$  mm horizontally and  $u_z = -253 \pm 10$  mm vertically. The  $u_r/u_z$  ratio of the cumulative displacements is  $2.03 \pm 0.09$  but scatter in the ratio is partly due to perturbations of the GPS signals by the plume (Supplementary Fig. 5). The co-eruptive tilt was  $\delta = 175 \pm 6$  µrad in the direction  $N35 \pm 6^\circ$  W, consistent with the GPS displacements. These deformation characteristics suggest that the signal is mostly due to a single source of fixed location and geometry throughout the eruption; a magma chamber with variable pressure.

<sup>1</sup>Nordic Volcanological Center, Institute of Earth Sciences, University of Iceland, IS-101 Reykjavík, Iceland, <sup>2</sup>Icelandic Meteorological Office, IS-150 Reykjavík, Iceland, <sup>3</sup>Geophysical Institute, University of Alaska, Fairbanks, Alaska 99775, USA, <sup>4</sup>The Pennsylvania State University, University Park, Pennsylvania 16802, USA, <sup>5</sup>University of Arizona, Tucson, Arizona 85721, USA, <sup>6</sup>EDYTEM, Université de Savoie/CNRS, F-73376 Le Bourget du Lac, France, <sup>7</sup>University of Gothenburg, SE-405 30 Gothenburg, Sweden. <sup>†</sup>Present addresses: GNS Science, Avalon 5010, Lower Hutt, New Zealand (S.H.); UC Berkeley Seismological Laboratory, Berkeley, California 94720, USA (R.G.). \*e-mail: runa@hi.is; fs@hi.is

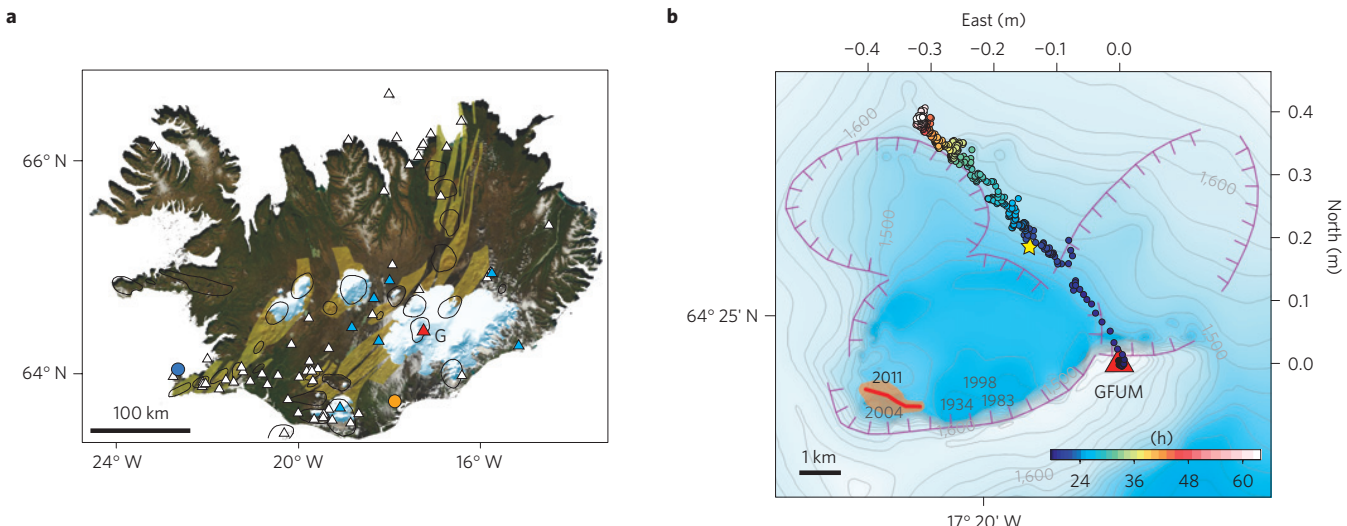


**Figure 1 | The location of Grímsvötn Volcano in Iceland and map of horizontal displacement.** **a**, CGPS stations (triangles; blue and red used in this study) and radars (blue circle C-band, orange circle X-band) in Iceland operating during the Grímsvötn (G) 2011 eruption. Pale green zones and black circles outline fissure swarms and central volcanoes. **b**, Caldera boundaries, 2011 eruptive fissure (area of ice melt indicated in brown), and the GPS station and tiltmeter on Mount Grímsfjall (GFUM, red triangle). North versus east component of the horizontal displacement, with colour scale giving timing of displacement relative to 0:00 UTC on 21 May. Star indicates the centre of the inferred magma chamber.

Deformation due to a subsurface magma source depends on the horizontal distance from the centre of the source,  $r$ , and its depth,  $d$ . The temporal evolution of surface deformation during eruptions reflects variations in overpressure within the magma source. Here we fit our geodetic observations with the Mogi model, widely used for a magma chamber: a point source of pressure within a homogeneous elastic half-space<sup>11,12</sup>. The model is characterized by a strength parameter,  $C$ , given by

$$C = \frac{3a^3}{4\mu} \Delta P \quad (1)$$

where  $a$  is the chamber radius and  $\mu$  is the modulus of rigidity for the elastic half-space. The Mogi model has four free parameters ( $C$  and three for location), which creates a challenge for the source estimation when observations are spatially limited to a single location (as in our case). The co-location of a GPS and a tiltmeter does, however, make this feasible and together the instruments act as a magma chamber meter. The magma chamber is located in the direction indicated by the combined measurements. Three observables ( $u_r$ ,  $u_z$  and  $\delta$ ) allow the determination of the remaining three model parameters referred to earlier:  $r$ ,  $d$  and  $C$ . Displacements are such that on the surface of the Earth  $u_r/u_z = r/d$ . The strength parameter can be related to observations by (Supplementary Methods):

$$C = 9 \frac{u_z^3}{\delta^2} \frac{(u_r/u_z)^2}{\sqrt{1 + (u_r/u_z)^2}} \quad (2)$$

We estimate the model parameters with two approaches giving similar results (Table 1 and Supplementary Methods). From the onset of immediate pre-eruptive deformation to its maximum at the end of 23 May, we find  $C = (9 \pm 1) \times 10^6 \text{ m}^3$ ,  $r = 3.5 \pm 0.2 \text{ km}$ , and  $d = 1.7 \pm 0.2 \text{ km}$ . The radial horizontal distance of GFUM to the centre of the source is twice the source depth, suggesting that the point source approximation is reasonable<sup>13</sup>. The model predicts about 6 mm co-eruptive signal at the next continuous GPS (CGPS) station (DYN $\ddot{\text{C}}$ ), at 43 km distance, in agreement with measurements ( $8 \pm 2 \text{ mm}$ ; Supplementary Fig. 2). The feeder, linking the magma chamber to the eruptive craters, evolves for

about 60 min before it breaches the Earth's surface. Only negligible effects from the feeder are detected in the form of a small transverse component of displacement before the eruption onset (Fig. 2).

Two weather radars monitored the height of the volcanic plume during the eruption (Figs 1a and 3a); a C-band radar located at Keflavík Airport, 257 km from the volcano, and a mobile X-band radar stationed 75 km from the volcano about 8.5 h after the eruption onset<sup>14</sup>. The radars resolved the height of the plume in steps as they scan the airspace with discrete beam elevation angles. Over the eruption site the stepping resulted in height resolution of 5 km above 10 km elevation for the C-band radar and 2–3 km for the X-band. Photographs show the plume ascent to 16 km altitude during the first ~30 min of the eruption<sup>14</sup> (Fig. 3a). A strong initial plume was followed by declining, pulsating activity. Between 19:21 on 21 May and 17:35 on 22 May, the measured plume height was often 15 km or more, with peaks at 20–25 km between 21:25 on 21 May and 06:40 on 22 May. Averages of the available plume height data over 30-min were used to generate a continuous curve of the plume elevation<sup>14</sup> (Fig. 3a).

Numerous studies have shown that plume height in explosive eruptions is a function of magma discharge<sup>2,3</sup>. An often-used empirical equation  $H = 2.0Q^{0.241}$  relates the plume height,  $H$ , to the magma flow rate,  $Q$ , in  $\text{m}^3 \text{s}^{-1}$  DRE (ref. 3). The result of direct integration of  $Q$  (magma discharge) with time, inferred from this equation, yields a DRE total volume of  $0.18 \text{ km}^3$ . By scaling the calculated discharge with the ratio of the mapped tephra volume and volume obtained by integrating  $Q$  with time (ratio =  $0.27/0.18 = 1.5$ ), the uncertainty in plume-derived magma discharge is significantly reduced<sup>15</sup>. The resulting estimate of magma flow rate (Fig. 3b) indicates that most of the tephra was erupted in the first 24 h (average discharge rate  $\sim 3,000 \text{ m}^3 \text{s}^{-1}$  or  $\sim 0.8 \times 10^7 \text{ kg s}^{-1}$ ). Variations in the slope of the curve indicate considerably higher discharge during intense plume pulses.

The rate of pressure drop in a magma chamber can be inferred from geodetic measurements using the Mogi model as  $C$ , and hence  $\Delta P$  (equation (1)), scales directly with changes in deformation. During the Grímsvötn eruption, the geodetically inferred ratio  $\Delta P/\Delta P_{\text{total}}$  shows the same temporal variations as the integrated magma flow estimated from plume height (Fig. 3b). Not only is the broad exponential decay very similar, smaller excursions also

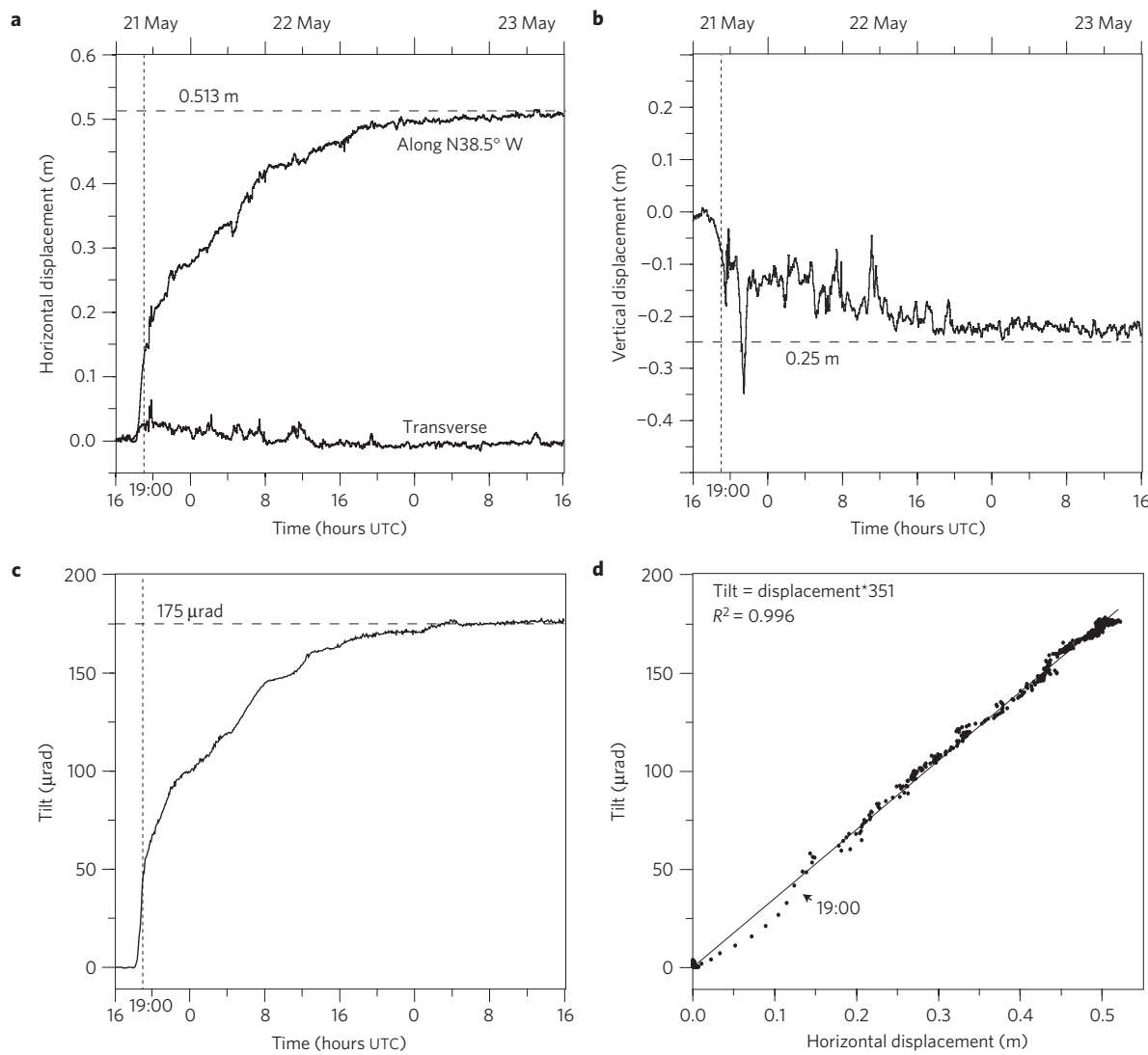


**Figure 2 | GPS and tilt time series 21–23 May 2011.** **a**, Horizontal displacements in direction N38.5° W and transverse to it. **b**, Vertical displacements. **c**, Ground tilt in direction N35° W. **d**, Tilt versus horizontal displacement, illustrating strong correlation of the parameters. The straight line corresponds to tilt (in  $\mu\text{rad}$ ) = 351  $\times$  displacement (in metres). The vertical lines mark the estimated onset of the eruption at 19:00. Horizontal lines mark the inferred total change during the eruption, reached near midday on 23 May. Thereafter (not shown), a slight reversal of trends occurs indicating slight pressure build up, despite the eruption continuing at a low rate until 28 May.

**Table 1 | Inferred magma chamber model parameters.**

Source parameter	Direct estimate	Markov chain Monte Carlo estimation
Strength, C	$(9 \pm 1) \times 10^6 \text{ m}^3$	
Depth, d	$1.7 \pm 0.2 \text{ km}$	1.6–1.9 km
Horizontal distance from GPS site, r	$3.5 \pm 0.2 \text{ km}$	
Latitude (° N)		64.431–64.433
Longitude (° W)		17.310–17.314
Total volume change of Mogi source, $(4/3)\pi C$	$(0.038 \pm 0.004) \text{ km}^3$	$(0.035–0.043) \text{ km}^3$
Co-eruptive volume change of Mogi source	$(0.75 \pm 0.01) \times (0.038 \pm 0.004) \text{ km}^3 = (0.027 \pm 0.003) \text{ km}^3$	
Volume of eruptive material inferred from tephra fallout (DRE)	$0.27 \pm 0.07 \text{ km}^3$	

Model parameters inferred directly with application of equation (2) on the observed deformation and subsequent equations from Supplementary Methods. Uncertainties on derived parameters are found by propagating the uncertainty of the observations. Also shown (far-right column) are model parameters estimated from formal inversion/probability density estimates by Markov chain Monte Carlo sampling (95% confidence intervals). See Supplementary Methods for details and inferred probability distributions. The range for derived parameters bracket the 95% confidence interval.

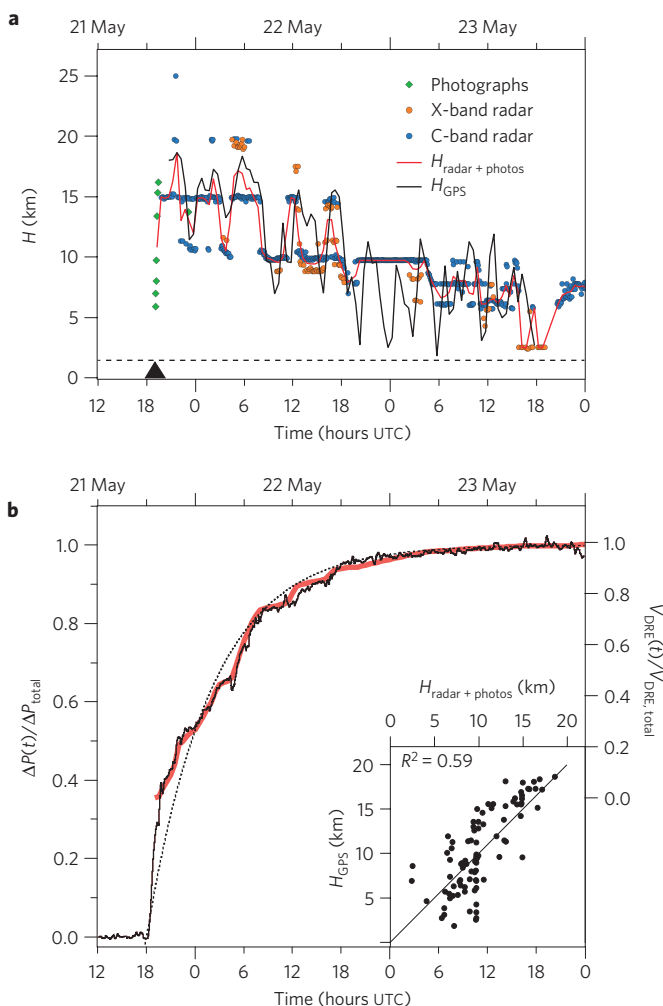


**Figure 3 | Plume-top altitude, pressure change and accumulated erupted volume as a function of time 21–23 May 2011.** **a**, Plume height based on radar measurements and photographs (red line 30 min average)<sup>14</sup> and inferred plume height from the GPS measurements (black line 60 min average). The dashed line marks the vent elevation (1.45 km). **b**, Change in pressure in the Grímsvötn magma chamber inferred from GPS measurements. It follows approximately an exponential decay with a decay time of 8 h (dotted line). The red line shows the normalized accumulated DRE erupted volume inferred from integrated plume-height data<sup>14</sup>. The inset shows the correlation between the 30-min average plume-top altitude versus the inferred 60-min average plume height based on GPS data.

correlate between both time series. The geodetic model gives an estimate of volumetric magma flow rate from the magma chamber,  $Q$  (refs 16,17). It scales with the rate of pressure decrease  $d\Delta P/dt$  as

$$Q = -\pi \left( \frac{1}{\mu} + \frac{4}{3k} \right) a^3 \frac{d\Delta P}{dt}$$

with  $1/k$  equal to the effective magma compressibility ( $k$  is the bulk modulus, Supplementary Methods). Using the empirical relationship between the volcanic plume height and magma flow rate, the plume height can be derived from the pressure drop in an underlying magma chamber,  $H \propto (d\Delta P/dt)^{0.241}$ . We use filtered GPS time series to estimate the evolution of the plume height (Fig. 3a), scaling it to match the 30-min average observations during the initial peak in activity (21:45). The evolution of the inferred plume height (60-min average) correlates closely with observation in the first 24 h (Fig. 3a). The estimated plume height shows pulsating behaviour

as suggested by radar measurements, with peaks exceeding 15 km height in the first 12 h, followed by a decline. After 24 h the measured plume height drops to 10 km or lower. GFUM reached maximum offset after about 48 h but the radar measurements indicate a fluctuating plume, below 10 km, and intermittent explosions with minor tephra fallout until the eruption ended on 28 May (ref. 14).

For the 2011 Grímsvötn eruption, the cumulative DRE volume of eruptive products is  $\Delta V_{\text{magma}} = (0.27 \pm 0.07) \text{ km}^3$ , but the geodetically derived co-eruptive chamber volume change is  $(0.027 \pm 0.003) \text{ km}^3$  (Table 1), giving a volume ratio of  $10 \pm 3$ . Effects of host rock rigidity and magma compressibility may, at least in part, explain this difference in volume estimates. Magma accumulating in the magma chamber compresses with increased pressure and during eruption magma remaining in the chamber expands<sup>18–20</sup>. The ratio for Grímsvötn 2011 is similar to the high end of previously obtained values. Figure 3b reveals similarity of the erupted volume curve and pressure change curve for the eruption as inferred from the GPS displacements. This implies that for this eruption geodetic displacements scale with eruptive flux. Constant scaling implies that the compressibility of the magma remaining in the shallow chamber did not evolve with time after the eruption breached the surface<sup>17</sup>. It argues against significant variations in exsolution of volatiles in magma residing in a magma chamber during an eruption, as this would change the compressibility<sup>19</sup>. It also implies relatively simple system dynamics and no changes in the effective magmatic plumbing of the volcano, such as new dykes or sills intruding a magma chamber, or magma mixing, as in such cases the scaling ratio would break down.

The excellent correspondence between volcanic plume heights during the Grímsvötn eruption and the rate of pressure change in the magma chamber indicates that high-rate GPS observations could be used to advance physics-based eruption models<sup>20</sup>. The initial pressure drop preceded the eruption by an hour but during the eruption we find constant scaling between the eruptive flux and the geodetic station velocity. If interpreted in near-real time, these observations could greatly improve forecasting of the onset and evolution of explosive eruptions and volcanic plume height. Implementation of our method would help improve the source term for volcanic plume dispersion models for the benefits of air traffic hazard management in future eruptions.

## Methods

The maximum co-eruptive change of GFUM was estimated from 8 h solutions analysed using GAMIT/GLOBK 10.4 (ref. 21) with 51 global CGPS stations realizing a fixed ITRF05 reference frame. The maximum co-eruptive change was obtained at the end of 23 May (Supplementary Table 1 and Fig. 2). Significant co-eruptive displacement ( $8 \pm 2$  mm towards the south) was observed at one other CGPS station, DYNC, 43 km north of Grímsvötn. Other sites had 3 mm or less co-eruptive displacement.

The kinematic trajectory of GPS station GFUM was estimated using the TRACK module of the GAMIT/GLOBK software<sup>21</sup>, with respect to base stations with no significant co-eruptive signal. Multi-path effects were reduced by sidereal filtering<sup>22</sup>, subtracting solutions from 20 May using the most common orbit repeat time of 24 h minus 246 s (ref. 23). To improve the signal-to-noise ratio, we averaged time series for GFUM estimated from seven different base stations at distances between 48 and 120 km. After the onset of the eruption we see an increase in r.m.s. misfit of the GPS time series. Oscillations in the vertical component can be explained by signal loss from some satellites and/or phase delay due to the presence of the eruption plume (Supplementary Methods).

The tiltmeter detects variations in tilt electrically using an air bubble within a glass tube. As the sensor tilts, changes in electrical resistance occur. The signal is then converted into a measurement of magnitude and direction of tilt. The raw streams from the tiltmeter were digitized and then transmitted. The north-south tilt component is resolved at 100 Hz with 22-bit resolution. The east-west component was sampled only at 4 Hz with 16-bit resolution. Artificial spikes and offsets resulting from digitization were resolved (Supplementary Methods).

When estimating the plume height from the GPS data we applied a one hour robust regression filter (rlowess Matlab function) to the horizontal GPS data, using weighted linear least squares and a first-degree polynomial model, and then differentiated with time. Using the empirical relationship between the

volcanic plume height (km) and magma flow rate<sup>3</sup>, the resulting site velocity ( $\text{m s}^{-1}$ ) was raised to the power of 0.241 and scaled. The scaling factor is dependent on the magma compressibility ( $1/k$ ), the modulus of rigidity for the elastic half-space ( $\mu$ ), the depth ( $d$ ) and the horizontal distance ( $r$ ) to the source. Here we used the first few hours of the measured plume height to evaluate a scaling factor of 287 to constrain the geodetically derived plume height, correcting for the vent elevation of 1.45 km. For a source depth of 1.7 km and radial distance 3.5 km this scaling factor corresponds to  $\mu/k \sim 6$ , which agrees well with the ratio implied by the geodetically derived co-eruptive chamber volume changes versus measured eruptive volume,  $\mu/k = 7 \pm 3$  (Supplementary Discussion). Uncertainty analysis shows that uncertainty in the estimated plume height due to analytical errors scales inversely in a nonlinear manner with the height; the uncertainty in the estimated plume height increases by a factor of 9 for a height reduction of 50%.

The geodetic time series presented in the paper are archived and accessible through the FUTUREVOLC website, <http://futurevolc.hi.is>.

Received 2 May 2013; accepted 21 November 2013;  
published online 12 January 2014

## References

- Dzurisin, D. *Volcano Deformation, Geodetic Monitoring Techniques* (Springer, 2007).
- Sparks, R. S. J. *et al.* *Volcanic Plumes* (Wiley, 1997).
- Mastin, L. G. *et al.* A multidisciplinary effort to assign realistic source parameters to models of volcanic ash-cloud transport and dispersion during eruptions. *J. Volcanol. Geotherm. Res.* **186**, 10–21 (2009).
- Björnsson, H. & Guðmundsson, M. T. Variations in the thermal output of the subglacial Grímsvötn Caldera, Iceland. *Geophys. Res. Lett.* **20**, 2127–2130 (1993).
- Alfaro, R., Brandsdóttir, B., Rowlands, D. P., White, R. S. & Guðmundsson, M. T. Structure of the Grímsvötn volcano under the Vatnajökull icecap. *Geophys. J. Int.* **168**, 863–876 (2007).
- Guðmundsson, M. T. & Milsom, J. Gravity and magnetic studies of the subglacial Grímsvötn volcano, Iceland: Implications for crustal and thermal structure. *J. Geophys. Res.* **102**, 7691–7704 (1997).
- Oddsson, B., Guðmundsson, M. T., Larsen, G. & Karlssdóttir, S. Monitoring of the plume from the basaltic phreatomagmatic 2004 Grímsvötn eruption—application of weather radar and comparison with plume models. *Bull. Volcanol.* **74**, 1395–1407 (2012).
- Sturkell, E., Einarsson, P., Sigmundsson, F., Hreinsdóttir, S. & Geirsson, H. Deformation of Grímsvötn volcano, Iceland: 1998 eruption and subsequent inflation. *Geophys. Res. Lett.* **30**, 1182 (2003).
- Sturkell, E. C. *et al.* Deformation cycle of the Grímsvötn sub-glacial volcano, Iceland, measured by GPS. *Am. Geophys. Fall Meeting abstr.* V31H-04 (2012).
- Sigmundsson, F. *Iceland Geodynamics, Crustal Deformation and Divergent Plate Tectonics* (Springer, 2006).
- Mogi, K. Relations between the eruptions of various volcanoes and the deformation of the ground surface around them. *Bull. Earthq. Res. Inst. Univ. Tokyo* **36**, 99–134 (1958).
- Segall, P. *Earthquake and Volcano Deformation* (Princeton Univ. Press, 2010).
- McTigue, D. F. Elastic stress and deformation near a finite spherical magma body: Resolution of the point source paradox. *J. Geophys. Res.* **92**, 12931–12940 (1987).
- Petersen, G. N., Bjornsson, H., Arason, P. & von Löwis, S. Two weather radar time series of the altitude of the volcanic plume during the May 2011 eruption of Grímsvötn, Iceland. *Earth Syst. Sci. Data* **4**, 121–127 (2012).
- Guðmundsson, M. T. *et al.* Ash generation and distribution from the April–May 2010 eruption of Eyjafjallajökull, Iceland. *Sci. Rep.* **2**, 572 (2012).
- Sigmundsson, F., Einarsson, P. & Bilham, R. Magma chamber deflation recorded by the Global Positioning System: The Hekla 1991 eruption. *Geophys. Res. Lett.* **19**, 1483–1486 (1992).
- Segall, P. Volcano deformation and eruption forecasting. *Geol. Soc. Lond. Spec. Publ.* **380** (2013).
- Mastin, L. G., Roeloffs, E., Beeler, N. M. & Quick, J. E. In *A Volcano Rekindled: The Renewed Eruption of Mount St. Helens, 2004–2006: Constraints on the Size, Overpressure, and Volatile Content of the Mount St. Helens Magma System from Geodetic and Dome-growth Measurements During the 2004–2006 + Eruption* (eds Sherrod, D. R. *et al.*) 461–492 (USGS Professional Paper 1750, US Geological Survey, 2008).
- Huppert, H. E. & Woods, A. W. The role of volatiles in magma chamber dynamics. *Nature* **420**, 493–495 (2002).
- Anderson, K. & Segall, P. Physics-based models of ground deformation and extrusion rate at effusively erupting volcanoes. *J. Geophys. Res.* **116**, B07204 (2011).
- Herring, R. T. A., King, W. & McClusky, S. C. GAMIT/GLOBK Reference Manuals, Release 10.4 (MIT Technical Reports, 2010).
- Larson, K. M., Bilich, A. & Axelrad, P. Improving the precision of high rate GPS. *J. Geophys. Res.* **112**, B05422 (2007).
- Agnew, D. C. & Larson, K. M. Finding the repeat times of the GPS constellation. *GPS Sol.* **11**, 71–76 (2007).

## Acknowledgements

We gratefully acknowledge the efforts of volunteers of the Icelandic Glaciological Society who operate the field research station at Mount Grímsfjall on Vatnajökull, and the technicians and staff at our institutions who have been involved in ensuring the successful collection of the data this paper is based on. Support for this work was received from the Icelandic Research Fund, the research fund at University of Iceland, National Science Foundation, USA, the French Polar Institute (IPEV Arctic program 316) and European Community's FP7 Programme Grant No. 308377 (Project FUTUREVOLC). The mobile X-band radar was on loan from the Italian Civil Protection Agency. We thank UNAVCO for technical support. GMT public domain software was used for some figures. T. Högnadóttir prepared the map on Fig. 1b. R.G. acknowledges support from the Alaska Volcano Observatory.

## Author contributions

S.H. and F.S. coordinated the writing of the paper and the research it is based on; S.H. and R.G. analysed the GPS data; M.J.R., S.H. and F.S. analysed the tilt data; M.T.G., B.O., Á.H., G.L., T.T. and B.A.Ó. measured and evaluated the volume of the eruptive products; H.B. and P.A. measured the plume height from radar data and photos and evaluated variations in eruption rate; M.J.R. analysed the seismic data; S.H., M.J.R., F.S., M.T.G., B.O., P.A. and Á.H. were involved in daily monitoring of the eruptive activity; J.H. was the lead person in engineering and installing the tilt and GPS station at Grímsfjall; H.G., S.H., R.A.B., T.V., E.S., T.Á., B.G.Ó. and T.J. supervised and led the installation and operation of the high-rate GPS stations used in the research; F.S. and T.Á. modelled the geodetic displacements; S.H. produced the paper figures; S.H., R.G., M.J.R. and T.Á. produced Supplementary figures; S.H., F.S., R.G., M.J.R., T. Á. and M.T.G. led the writing of the paper with all authors discussing the results and commenting on the manuscript.

## Additional information

Supplementary information is available in the online version of the paper. Reprints and permissions information is available online at [www.nature.com/reprints](http://www.nature.com/reprints). Correspondence and requests for materials should be addressed to S.H. or F.S.

## Competing financial interests

The authors declare no competing financial interests.